Protein Folding Intermediates with Rapidly Exchangeable Amide Protons Contain Authentic Hydrogen-Bonded Secondary Structures†

J. Iñaki Guijarro,‡ Michael Jackson,‖ Alain F. Chaffotte,§ Muriel Delepierre,‡ Henry H. Mantsch,‖ and Michel E. Goldberg*,§

Laboratoire de Résonance Magnétique Nucléaire and Unité de Biochimie Cellulaire, Institut Pasteur, 28 rue du Dr. Roux, 75724 Paris Cedex 15, France, and Institute for Biodiagnostics, National Research Council Canada, 435 Ellis Avenue, Winnipeg, Manitoba R3B 1Y6, Canada

Received September 26, 1994; Revised Manuscript Received January 3, 1995⊗

ABSTRACT: Recent studies on protein folding intermediates by pulsed amide proton exchange and by far-ultraviolet circular dichroism have shown important discrepancies between the secondary structure contents estimated by these two methods at early folding stages. To solve these apparent discrepancies, structural studies have been performed on the isolated, 101 residue long, C-terminal proteolytic domain (F2) of the *Escherichia coli* tryptophan synthase β chain, which had previously been reported to behave as an early folding intermediate [Chaffotte, A. F., Cadieux, C., Guillou, Y., & Goldberg, M. E. (1992) *Biochemistry 31,* 4303−4308]. The secondary structure of F2 has been investigated by far-UV circular dichroism (CD), Fourier transform infrared (FTIR) spectroscopy, and NMR. The CD and FTIR spectra clearly indicate that isolated F2 has about 30−45% of its residues involved in secondary structures stabilized by conventional hydrogen bonds. The characteristics of the NMR spectrum (line broadening, absence of structure-induced chemical shifts, absence of nuclear Overhauser effects in the amide region, few dipolar interactions between the side-chain protons) suggest that isolated F2 is oscillating between several conformations in rapid equilibrium. The rate of amide proton exchange has been studied by one-dimensional NMR, which indicates a significant extent of proton protection, with, however, protection factors that can be estimated to be at most 60 and more probably closer to 10. Thus, F2 appears to exist as a molten globule that exhibits very low amide proton protection and yet contains a large fraction of its residues involved in authentic secondary structures stabilized by hydrogen bonds. Such a state is likely to correspond to the earliest structured folding intermediates thus far characterized.

Recent studies on protein folding have led to the observation of early folding intermediates with far-UV circular dichroism spectra that reflect the presence of large amounts of secondary structure at a stage where pulsed proton exchange followed by NMR[1] analysis indicates the presence of no, or little, secondary structure. Thus, after 4 ms of refolding, only a small fraction of the backbone amide protons of hen egg white lysozyme was protected against exchange with protons from the solvent. Yet, at this stage of the folding process, a large fraction of the ellipticity at 222 nm was already regained (Radford et al., 1992). A time-resolved analysis of its far-UV CD spectrum in fact suggested that, within the first 4 ms of folding, lysozyme had already regained a native-like secondary structure (Chaffotte et al., 1992b). Similarly, during the refolding of cytochrome *c*, nearly 50% of the native far-UV CD spectrum was regained in 4 ms, while pulsed proton exchange experiments indicated the presence of only 10−15% of the native secondary structure at this early stage of the folding process (Elöve et al., 1992). A discrepancy between the amounts of secondary structure estimated by CD and by pulsed proton exchange was also reported during the refolding of interleukin-1β, for which 90% of the native far-UV ellipticity was present after 25 ms of folding, while protection of the amide protons began to appear only after 1 s (Varley et al., 1993).

These observations raise an apparent paradox. If the backbone conformation giving rise to the far-UV CD spectra of the early intermediates were authentic secondary structures, stabilized by hydrogen bonds, one would expect a large number of the peptide amide protons to be protected from exchange with solvent protons (Englander et al., 1972; Baldwin & Roder, 1991; Rohl et al., 1992; Baldwin, 1993). Why then does pulsed amide proton exchange followed by NMR identification of the slow-exchanging protons in the native protein show only marginal protection in these "CD rich" early folding intermediates? The present study was aimed at testing several hypotheses that could account for this apparent paradox. The three following models were considered:

(1) The optically active conformations detected by CD at early stages of the folding process would not be the classical

† This work was supported by funds from the Institut Pasteur, the Centre National de la Recherche Scientifique (URA 1129), the Paris 7 University, The Association Franco-Israelienne pour la Recherche Scientifique et Technique (AFIRST), and the National Research Council Canada. J.I.G. is a fellow of the Universidad Nacional Autónoma de México.

* To whom correspondence should be addressed.
‡ Laboratoire de Résonance Magnétique Nucléaire, Institut Pasteur.
§ Unité de Biochimie Cellulaire, Institut Pasteur.
‖ National Research Council Canada.

⊗ Abstract published in *Advance ACS Abstracts,* February 15, 1995.

[1] Abbreviations: ANS, 8-anilino-1-naphthalenesulfonic acid; CD, circular dichroism; DSS, sodium 4,4-dimethylsilapentane sulfonate; DTT, dithiothreitol; EDTA, ethylenediaminetetraacetic acid; FTIR, Fourier transform infrared spectroscopy; NMR, nuclear magnetic resonance; NOE, nuclear Overhauser enhancement; NOESY, nuclear Overhauser enhancement spectroscopy; 1D, 2D, and 3D, respectively one-, two-, and three-dimensional.

0006-2960/95/0434-2998$09.00/0

hydrogen-bonded α-helices or β-strands originally described by Pauling and Corey (1951a,b). Rather, they would result from an initial hydrophobic collapse of the protein that might produce non-hydrogen-bonded, repetitive backbone conformations endowed with a far-UV ellipticity resembling that of authentic secondary structures.

(2) Early folding intermediates would contain classical secondary structures that should indeed protect amide protons against exchange under the conditions where the folding occurs. But in the absence of stabilizing tertiary interactions, these secondary structure elements would be too labile to withstand the rather drastic pH jumps during the pulsed proton exchange (pH 9.5 or above, in most studies) or during the later phases of the analysis (pH down to about 3−5.5), thus leading to the release of the trapped protons.

(3) Early folding intermediates would contain authentic secondary structures which would fail to significantly protect the amide protons involved in their hydrogen bonds, due to a low stability of these secondary structures even under folding conditions or to a very rapid equilibrium between organized and random conformations.

Experiments to test these hypotheses are difficult because the intermediates of interest are, by nature, short lived. Thus, among the methods usually used to investigate protein structure, only pulsed proton exchange and CD stopped-flow can probe the presence of secondary structure rapidly enough, and as pointed out above, they yield conflicting results. Equilibrium intermediates in the reversible folding/unfolding transition of several proteins, corresponding to a state called the "molten globule", have been shown to share several structural features with kinetic intermediates observed at early stages of the folding process (Kuwajima, 1989; Jennings et al., 1993). But these equilibrium intermediates are stable only under destabilizing conditions that widely differ from those under which the protein can fold efficiently. Ideally, one would therefore like to "freeze" early folding intermediates under non-destabilizing conditions and investigate their structure by methods that would be slower, but complementary, to stopped-flow CD and pulsed proton exchange. This seemed possible in the particular case of the C-terminal proteolytic domain of the β_2 subunit of *Escherichia coli* tryptophan synthase. Each β chain can be cleaved by the staphylococcal protease V-8 between residues E-296 and S-297 (Friguet et al., 1989; Kaufmann et al., 1991), generating a 296-residue N-terminal fragment (F1) and a 101-residue C-terminal fragment (F2). The fragments can be separated from one another under denaturing conditions, and isolated F2 was shown to refold in the absence of F1 into an essentially monomeric, globular conformation (Chaffotte et al., 1991). Examination of the 3D structure of the $\alpha_2\beta_2$ tryptophan synthase complex (Hyde et al., 1988) shows that, in the native protein, each F2 fragment makes most of its tertiary contacts either with the other F2 or with the F1 fragments within the dimer. It was therefore predicted that, if allowed to fold in the absence of F1, the F2 fragment should be blocked at the stage of the molten globule because it is unable to make the tightly packed tertiary contacts that are required to drive the polypeptide chain into the native state. This prediction was amply verified (Chaffotte et al., 1991). Indeed, isolated F2 was shown to exhibit under "native" conditions the following characteristics of a molten globule: a Stokes radius compatible with a collapsed, but not compact, globular structure; a large far-UV CD signal indicating the presence of large amounts of secondary structure; no near-UV ellipticity, which shows the absence of defined tertiary structure near the aromatic side chains; no detectable induced chemical shift in the NMR spectrum, confirming the absence of tertiary contacts; no strong protection of protons against exchange with the solvent; ANS binding, which indicates the presence of a solvent-accessible hydrophobic core; and a non-cooperative thermal transition, with an unusually high T_m (about 70 °C) and a very low enthalpy of denaturation (Chaffotte et al., 1991, 1992a). Moreover, fluorescence and CD stopped-flow studies showed that this stable, molten globular state was reached by F2 in less than 4 ms of folding (Chaffotte et al., 1992a), indicating that this state of F2 exhibited the usual characteristics of the early intermediates identified during the folding of a variety of proteins. Isolated F2 thus appeared as a good experimental model to investigate the discrepancy in the amounts of secondary structure detected by far-UV CD and by pulsed proton exchange at early stages of protein folding.

We shall show that the far-UV CD spectrum of isolated F2 is not significantly affected by increasing the pH to 9.5, which indicates that the secondary structure of F2 is stable under the conditions of a pulsed proton exchange experiment. We shall report a Fourier transform infrared analysis demonstrating that isolated F2 contains authentic hydrogen-bonded secondary structures in amounts compatible with those estimated from the CD spectrum. Finally, we shall report a quantitative analysis by NMR of proton exchange rates in isolated F2, which showed low protection for the amide protons of F2 at neutral pH, with protection factors so small that little proton protection would be expected in a pulsed exchange experiment. The reasons why pulsed proton exchange and NMR fail to detect these secondary structures will be discussed.

MATERIALS AND METHODS

Chemicals and Buffers. Unless otherwise stated, all CD and FTIR experiments were performed in buffer A (20 mM potassium phosphate, pH 7.8, and 5 mM β-mercaptoethanol). NMR and analytical centrifugation experiments were carried out in buffer B (20 mM potassium phosphate, pH 7.8, 0.4 mM sodium EDTA, and 0.4 mM DTT). When needed, the buffer was prepared with D_2O (99.9%, from the CEA−Saclay, France) by dissolving the desired amount of nonenriched salts and adjusting the pH with 1 N potassium hydroxide. No correction for the isotope effect was applied to the pH meter reading.

The endoproteinase Glu C from *Staphylococcus aureus* strain V8 was purchased from Boehringer. All other chemicals were reagent grade from standard commercial sources.

Preparation of F2. Isolated F2 was prepared by proteolysis of the β_2 subunit of *E. coli* tryptophan synthase with the endoproteinase Glu C as described previously (Chaffotte et al., 1991). The concentration of F2 was determined by measuring the absorbance at 280 nm, using an extinction coefficient of 0.37 $(mg/mL)^{-1}$ cm^{-1} at pH 7.8 determined through the quantitative amino acid analysis of an F2 solution of known absorbance. When solutions at a different pH were prepared, the protein concentration was determined by the method of Bradford (1976), using a solution of F2 at pH 7.8 as a standard.

CD Spectra. CD spectra were recorded in a Jobin-Yvon (Longjumeau, France) CD6 spectrodichrograph, using a 0.2-mm path length cell. The temperature was 20 °C. The wavelength region scanned was between 185 and 255 nm. The spectral bandwidth was kept at 2 nm, the wavelength increment was 0.2 nm per step, and the accumulation time was 1 s per step. Each spectrum resulted from averaging five successive individual spectra. The spectrum of the solvent alone was recorded under identical conditions and substracted from the sample spectrum to generate the protein contribution to the CD spectrum. The secondary structure content was estimated according to the method of Hennessey et al. (1981) with variable selection of protein spectra from a 22-spectra basis (Manavalan & Johnson, 1987), using the VARSLC1 program.

Fourier Transform Infrared Spectroscopy. A stock solution of F2 (12 mg/mL) in deuterated buffer A was prepared by a 24-h dialysis at 4 °C, with three buffer changes against buffer A prepared in D_2O. Infrared spectra were recorded at 20 °C on a Digilab FTS40A (Bio-Rad, Cambridge, MA) Fourier transform infrared spectrometer equipped with a liquid nitrogen cooled MCT detector and continuously purged with dry air. Protein solutions (5 μL) were placed between a pair of calcium fluoride windows separated by a 50-μm Mylar spacer and mounted in a Harrick cell. For each sample 1024 scans were recorded, coadded, and Fourier transformed to generate a spectrum of 2 cm^{-1} nominal resolution. A buffer spectrum was recorded under identical conditions and interactively subtracted to yield the protein spectrum. Residual water vapor was also interactively subtracted.

Analytical Ultracentrifugation. Centrifugation was performed in an XLA (Beckmann) analytical ultracentrifuge using 12-mm optical path cells with aluminium-filled double-sector center pieces and quartz windows. F2, dialyzed against buffer B, was heated for 10 min at 80 °C just before the start of the centrifugation. Its concentration was 2.7 mg/mL as determined from the absorption spectrum, which showed no evidence of scattered light and hence of aggregates. One hundred microliters of protein solution was layered over 75 μL of FC43 fluorocarbon in the sample sector, which resulted in a 2.5 mm high solution column. The reference sector was filled with 50 μL of FC43 and 150 μL of buffer. The centrifugation was conducted at 20 °C. Sedimentation/diffusion equilibrium was achieved after 24 h of sedimentation at 20 000 rpm. After the absorbance in the cell was scanned at 286 nm, the rotor was further accelerated to 40 000 rpm to deplete the protein at the meniscus and obtain the value of the base line. The data recorded at equilibrium were analyzed by means of the DATA-RED software provided with the XLA centrifuge. Three different fitting programs were tried, which rely on the three following models: an ideal solution with one solute molecule of molecular weight 11 kDa; an ideal solution with two solute molecules, one of molecular weight 11 kDa and the other with a molecular weight to be fitted; and an association−dissociation equilibrium between monomers, dimers, trimers, and tetramers, with a monomer molecular weight of 11 kDa. In all fittings, the base line was allowed to vary and was compared to the value of the base line obtained after meniscus depletion at 40 000 rpm. The partial specific volume of F2 was taken to be 0.73 cm^3/g, and the solvent density was taken to be 1 g/cm^3.

NMR Spectra and Amide Proton Exchange. All NMR experiments in H_2O were carried out in buffer B containing 10% D_2O. The pH was adjusted to 7.8 at 22 °C. F2 samples at pH 7.0 (22 °C) were prepared by adding 0.5 N HCl to pH 7.8 samples under vortexing to avoid the precipitation of the protein due to drastic variations in local pH; F2 was then centrifuged for 30 min at 4 °C and 17600*g* to eliminate possible aggregates. For experiments in D_2O, F2 was extensively dialyzed at 4 °C against 50 mM ammonium bicarbonate, pH 7.8, and then lyophilized. Unless stated otherwise, NMR experiments were done at 0 °C. pH was measured for each sample at the temperature of the experiment. Protein concentrations were kept relatively low to ensure that F2 was essentially in a monomeric form, and they typically ranged from 0.28 to 0.85 mM. Exchange kinetics in D_2O were done at a lower concentration (0.1 mM) to reduce aggregation problems following F2 lyophilization. CD spectra were acquired for each sample before and after NMR experiments to check the stability of the F2 fragment.

NMR spectra were recorded on a Varian Unity 500-MHz spectrometer equipped with a Sun Sparc 2 station. Data were processed with the Vnmr software (Varian Inc.). DSS was used as an external reference. Spectra were recorded with a sweep width of 4800 or 5400 Hz (1D) and 5000 Hz (2D).

NOESY spectra were recorded at 0 °C with a 120-ms mixing time. Water suppression was achieved with a combination of short hard pulses and spin-lock pulses (Sodano & Delepierre, 1993a). The delay between 90° pulses and the spin-lock pulse was adjusted to 149 μs to obtain maximum excitation at 8.5 ppm. Each free induction decay consisted of 2048 complex data points, zero filled to 4096, and 48 scans were collected. A total of 512 complex points were acquired in the t_1 dimension and were extended to 1024 with zero filling. The time-domain data were multiplied by a shifted sine square function before Fourier transformation.

Proton exchange rates were measured in D_2O and in H_2O. Amide exchange in D_2O buffer was initiated by dissolution at 0 °C of lyophilized F2 in buffer B prepared in 99.8% D_2O (the final pD value was 7.4 at 0 °C). NMR spectra were recorded directly after dissolution to follow the decrease in intensity of amide proton resonances.

As no NH proton signal could be observed even in the first recorded spectrum (see Results), amide exchange rates could not be directly determined. To obtain a lower limit for the amide exchange rate, it was necessary to estimate the minimum intensity that would have been observed under the experimental conditions used, and to determine the initial intensity (i.e., the expected signal before the exchange started) in terms of proton number or fraction at any chemical shift. The minimum observable intensity in the "exchanged" spectrum was set to be equal to the maximum noise level. The initial intensity was estimated by calculating the number of protons at a given frequency in an 11-echo spectrum in H_2O and taking as reference the peak height of the Tyr $H_{3,5}$ signal (6 protons). Appropriate corrections for the excitation intensity profile of the 11-echo spectrum were done. The lower limit for the amide exchange rate was then calculated assuming a single-exponential decay for the proton intensity.

In H_2O, the amide exchange rates were determined using the magnetization-transfer technique proposed by Spera and co-workers (1991). 1D spectra were recorded at pH 7.8 and 7.0 (pH measured at 22 °C) with and without water resonance

presaturation, under exactly the same conditions. Standard jump and return (Plateau & Guéron, 1982) and/or 11-echo (Sklenár & Bax, 1987) sequences were employed at 0, 20, and 25 °C. The "tau" delay between 90° pulses was set to obtain maximum excitation near the center of the amide region. Sweep time was 0.74 s. Presaturation was applied for 1.5 s during the relaxation time, and the field strength was adjusted to 18, 25, 36, 50, and 72 Hz. The intensity of the amide region envelope showed, within experimental error, to be independent of the field strength used for presaturation, indicating that a presaturation plateau was reached.

The intensity of amide protons in 1D spectra was evaluated by integration of the whole amide resonances envelope (9−7.8 ppm). The aromatic region (7.4−6.7 ppm) or the aromatic signal of Tyr residues was taken as reference. By measuring the intensity of almost all the amide protons we determined a "bulk" exchange rate at working pHs, with eq 1:

$$k_x = (M_o/M_{ps} - 1)/T_1^* \quad (1)$$

where k_x (in s^{-1}) is the bulk exchange rate determined experimentally at pH x, M_o and M_{ps} represent respectively the sum of the magnetization of all the amide protons in the spectrum without presaturation and with presaturation at pH x, and T_1^* is the mean apparent relaxation time of amide protons in the presence of exchange. According to Spera et al. (1991), the selective relaxation time in the absence of exchange with water (T_1) should be used to calculate exchange rates. However, F2 does not have any "slow"-exchanging amide, and so the measure of true selective T_1 relaxation times is not possible.

The contribution of cross relaxation to exchange rates calculated with eq 1 was taken into account by repeating the experiment at two different pH values. Resulting exchange rates were transposed to pH 7.8 (k_e) for each temperature with the following equation:

$$k_e = k_1 \times 10^{(7.8-pH_1)} \quad (2)$$

where k_1 is the bulk exchange rate at pH_1 in the absence of cross relaxation.

Amide proton apparent longitudinal relaxation times (T_1^*) were determined by the inversion−recovery method in buffer B. Repetition delays between scans and acquisition time were 8.4 and 1.6 s, respectively. Recovery times varied from 0 to 0.81 s. Ninety-six transients were acquired for each of the 28 recovery times. T_1^* values were calculated by fitting the intensities of 13 unresolved peaks to single-exponential decays.

Intrinsic exchange rates for individual amide protons were computed using the revised "Molday factors" and taking into account isotope effects for NH exchange in H_2O and D_2O as previously described (Bai et al., 1993; Connelly et al., 1993).

An upper limit for the detection of exchange rates (lim_{up}) was established with eq 1, considering that if the amide envelope intensity after presaturation was inferior to 5% of the intensity in the spectrum without presaturation ($M_o/M_{ps} \leq 20$), the signal would not be detected. Similarly, the lower limit (lim_{lw}) was established assuming that differences of 5% in the amide envelope intensity of the spectra with and without presaturation would not be detected accurately.

The bulk exchange rate that would be experimentally observed if none of the F2 protons were protected (k_{esu}), i.e., if they all exchanged at their intrinsic exchange rate, was predicted using the theoretical exchange rate (k_{th}^i) to calculate for each proton the intensity of its signal upon presaturation (M_{ps}^i):

$$M_{ps}^i = 1/([k_{th}^i T_1^*] + 1) \quad (3)$$

Then, we assumed that the signals of the 96 amide protons of F2 were included in the experimentally integrated region (9−7.8 ppm). This assumption is based on the fact that no NH−CαH is seen in the NOESY spectra at 0 °C outside the 9−7.8 ppm range. Finally, the value of k_{esu} was computed with eq 4:

$$k_{esu} = (96/M_{ps} - 1)/T_1^* \quad (4)$$

where M_{ps} is the summation of the M_{ps}^i obtained for each amide hydrogen.

The protection factor (P_1) that should be applied to the 96 amide protons of F2 to reproduce experimental bulk exchange rates was obtained from eq 5,

$$k_e = [96/\sum_i\{1/((k_{th}^i/P_1)T_1^* + 1)\} - 1]/T_1^* \quad (5)$$

which is algebraically derived from eqs 3 and 4 after replacing k_{esu} by k_e.

Similarly, P_2, the protection factor that should be applied to the 48 amide protons of F2 that are involved in helical structures within the context of the $\alpha_2\beta_2$ complex crystal (Hyde et al., 1988) to reproduce the experimental k_e values, was determined from eq 6:

$$k_e = [48/\sum_i\{1/(k_{th}^i T_1^* + 1)\} - 1]/T_1^* + [48/\sum_i\{1/((k_{th}^i/P_2)T_1^* + 1)\} - 1]/T_1^* \quad (6)$$

Here, 48 amides are supposed to exchange at their intrinsic exchange rates (first term in the equation) while the other 48 amide protons are supposed to be protected, with a protection factor equal to P_2 (second term in the equation).

RESULTS

CD Spectra and Secondary Structure Contents at pH 7.8 and 9.5. The far-UV CD spectrum of F2 at pH 7.8 was recorded as described in Materials and Methods and is shown in Figure 1. Analysis of this spectrum in terms of secondary structure provided the results reported in Table 1, which indicate that isolated F2 contains large amounts of secondary structure.

Figure 1 also shows the CD spectrum obtained after overnight dialysis of F2 at 4 °C against buffer A previously adjusted to pH 9.5. The spectra at pH 7.8 and 9.5 appear identical. Decomposition of the pH 9.5 spectrum provided the secondary structure estimates shown in Table 1. It can be seen that the estimated contents of α-helix and β-structure show no significant change between pH 7.8 and 9.5. This rules out the possibility that the pH jump during a pulsed proton exchange experiment disrupts the secondary structure of F2 and thus permits the exchange of protons that would have been protected at pH 7.8.

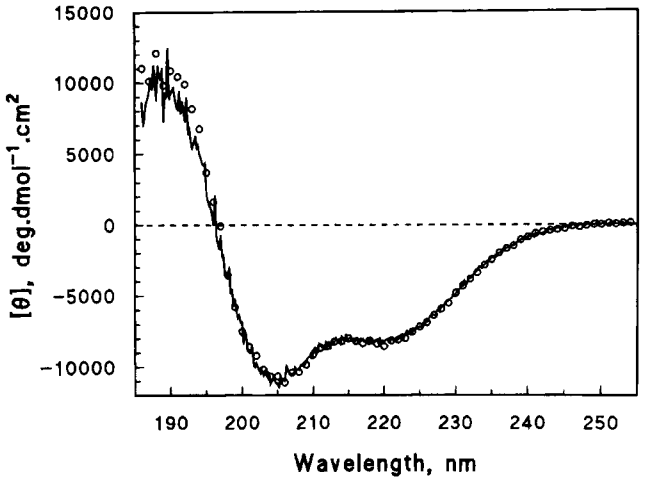

FIGURE 1: Far-UV circular dichroism spectra of F2 at pHs 7.8 (—) and 9.5 (○) at 20 °C. The F2 concentration was 0.5 mg/mL; the path length was 0.2 mm. The solvent was buffer A (pH 7.8) or buffer A adjusted to pH 9.5 by addition of concentrated potassium hydroxide. The mean residue molar ellipticity $[\theta]$ at each wavelength was obtained using the expression $[\theta] = 100\theta_{obs}/lc$, where θ_{obs} is the observed ellipticity in degrees, c is the molar residue concentration, and l is the light path in centimeters (Yang et al., 1986).

Table 1: Secondary Structure Content (%) of F2 Estimated by CD[a]

structure	pH 7.8	pH 9.5
α-helix	21	21
β-structure	23	22
turns	25	24
unordered	32	30
total	101	97

[a] Secondary structure content was predicted using the method of Hennessey and co-workers (1981) with variable selection of protein spectra basis (Manavalan & Johnson, 1987). Best fits were obtained with 18 proteins out of a 22-protein spectra basis. Selection criteria for best estimates were as follows: sum of fractions of secondary structure estimates between 0.96 and 1.05, no secondary structure estimate lower than −0.03, and root mean square error below 0.090.

Infrared Spectroscopy. Infrared spectra of proteins are dominated by the amide I band (essentially a secondary amide C=O stretching vibration). Discrete secondary structures within proteins are associated with characteristic hydrogen-bonding patterns, which in turn give rise to characteristic amide I bands. The position of amide I maxima can therefore provide information concerning protein secondary structure (Surewicz & Mantsch, 1988; Jackson & Mantsch, 1991). Unfortunately, the large width and small separation of these individual amide I bands result in considerable overlap such that a composite amide I band is usually seen. Application of mathematical routines such as Fourier self-deconvolution or Fourier derivation, which artificially narrow infrared absorption bands, allows visualization of overlapped bands, and assignment then becomes possible.

Figure 2 shows the infrared spectrum in the amide I region of F2 in deuterated buffer after Fourier self-deconvolution and Fourier derivation. After deconvolution the amide I maximum is seen at 1647 cm^{-1} with shoulders apparent at 1632 and 1676 cm^{-1} (Figure 2A). The position of the major absorption (1647 cm^{-1}) is intermediate between those usually found for polypeptide strands with no regular hydrogen-bonding pattern (unordered chains absorb at 1644 cm^{-1}) and for polypeptide chains which adopt an α-helical configuration

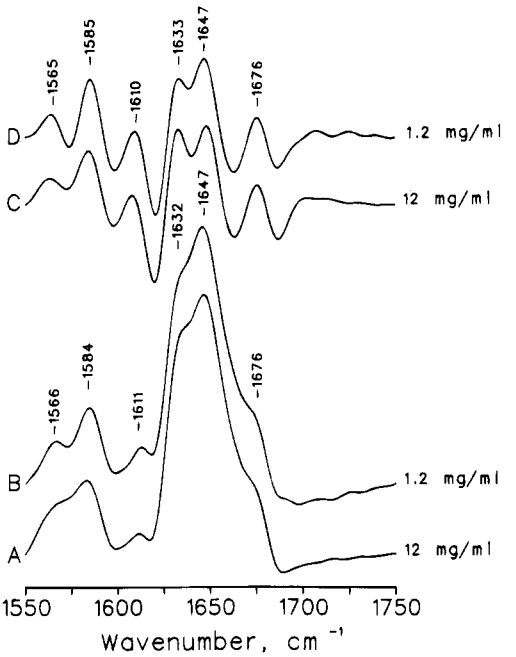

FIGURE 2: Infrared spectra of F2 in the amide I region. The absorbance of F2 at 12 mg/mL (A, C) and at 1.2 mg/mL (B, D) in buffer A prepared in D_2O (pD 7.8) was recorded at 20 °C. The spectra shown were obtained after Fourier self-deconvolution (A, B) and after Fourier derivation (C, D). Fourier self-deconvolution was performed as described previously (Cameron & Moffatt, 1984) using a half-width of 20 cm^{-1} and a band-narrowing factor of 2. A third-power Fourier derivative was calculated for each spectrum with a breakpoint of 0.18, which would correspond to a smoothed fourth derivative (Cameron & Moffatt, 1987).

(1650 cm^{-1}). This feature therefore represents overlapping absorptions assignable to irregular polypeptide chains and α-helices. An amide I band at 1632 cm^{-1} is indicative of the presence of β-sheet structures, while the remaining amide I band at 1676 cm^{-1} arises from turns. The presence of each of these features is confirmed by Fourier derivation, a more drastic band-narrowing technique (Figure 2C). The FTIR spectra therefore unambiguously confirm the presence of authentic hydrogen-bonded structures. The absorptions between 1560 and 1610 cm^{-1} arise from side-chain vibrations of glutamate, aspartate, arginine, and tyrosine.

The concentration required for FTIR spectroscopy is relatively high and may result in some molecular association of F2. A 10-fold dilution, under which conditions F2 is known to be monomeric (Chaffotte et al., 1991), produced spectra essentially identical to those obtained at high concentrations (Figure 2B,D). Some minor differences in the structure of the protein are suggested by a decrease in the relative intensity of the feature attributed to β-sheets (1632 cm^{-1}) upon dilution. In addition, some side-chain vibrations appear to be affected. This may reflect a small stabilization of β-sheets at high concentration together with subtle changes in the environment of some side-chain groups.

Quantitative estimates of the percentages of the various secondary structures present within F2 at each concentration obtained from a curve-fitting analysis of the amide I region are given in Table 2. While these numbers should not be taken as absolute values due to the various assumptions inherent in curve-fitting routines (equal molar absorptivities of secondary structures, failure to adequately compensate for side-chain absorptions, underestimation of the number of components to be fitted, etc.; see Surewicz et al., 1993), they

Table 2: Secondary Structure Content of F2 Estimated by FTIR

concn (mg/mL)	wavenumber (cm−1)	% area	assignment
12	1630.7	12.3	β-sheet
	1646.7	76.2	unordered/helices
	1672.9	11.5	turns
1.2	1630.4	8.1	β-sheet
	1645.7	80.5	unordered/helices
	1672.7	11.4	turns

can provide good estimates, particularly when used in a comparative manner. These reservations aside, the quantitative estimates show the involvement of at least 20−25% of amide C=O groups in hydrogen bonds typical of β-sheets and turns. A precise estimate of the helical content of the protein is difficult in this instance due to the overlap of helical and unordered absorptions. Interestingly, the suggestion of increased order at high protein concentrations is confirmed by the quantitative analysis; i.e., the β-sheet content is increased by 4% at the expense of helices and/or disordered structures (a shift to higher wavenumber of the absorption maximum of the major band in curve fitting of the concentrated solution suggests that the features lost are unordered structures).

Association/Dissociation Equilibrium. The molecular weight distribution of F2 at a concentration close to that used for FTIR and NMR experiments was investigated by sedimentation−diffusion equilibrium in an analytical ultracentrifuge. A solution of F2 in buffer B was heated at 80 °C for 10 min [see Chaffotte et al. (1991)]. Immediately after cooling, an aliquot was used to record the absorption spectrum, which showed no evidence of scattered light (and hence of large aggregates). The protein solution (2.7 mg/mL) was then introduced into a centrifugation cell and accelerated to 20 000 rpm. The absorption spectrum in the cell (at 6.85 cm from the rotation axis) was recorded between 250 and 400 nm as soon as the centrifugation speed was reached and 1 h later. The two spectra were superimposable and identical to that obtained in the spectrophotometer. This indicated that high molecular weight aggregates were not present in the solution. The centrifugation speed was kept at 20 000 rpm for 24 h. At this time, sedimentation−diffusion equilibrium was reached as judged by comparing several successive scans made at 90-min intervals. The concentration distribution at equilibrium was analyzed by means of the software supplied with the XLA centrifuge. The best fit was obtained using the two-component ideal solution model (see Materials and Methods). The χ^2 was 0.000 14, and the value of the fitted base line (0.097) was very close to that obtained by meniscus depletion at 40 000 rpm (0.102). The fitted curve is shown in Figure 3 together with the experimental data. According to these results, the protein solution would contain about 93% monomers and 7% oligomers with a molecular mass of about 70 kDa.

Though the results of this fitting should by no means be taken as a solid and exhaustive description of the association/dissociation equilibrium, they definitely show that a 2.7 mg/mL solution of F2 (0.24 mM) centrifuged during 24 h in the same buffer as that used for NMR studies (see below) contained essentially monomers.

NOESY Spectrum at pH 7.8. The 2D NOESY spectra of F2 at three different concentrations (0.28, 0.61, and 0.85 mM) were recorded at 0 °C. They were superimposable. Because,

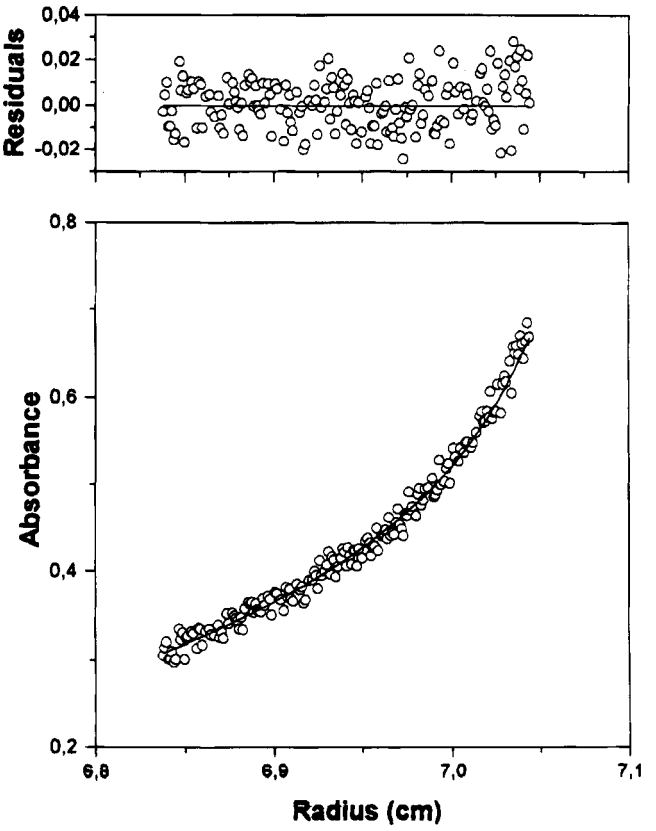

FIGURE 3: Sedimentation/diffusion equilibrium of F2 (0.24 mM). A solution of F2, initially at 2.7 mg/mL in buffer B, was sedimented to equilibrium at 20 °C and 20 000 rpm. The absorbance at 286 nm was scanned as a function of the distance to the rotation axis. Ten scans were accumulated. Lower panel: The experimental points (open circles) were used to generate a fitted curve (continuous line) using as a model an ideal solution with two solute molecules (see Materials and Methods). Upper panel: Plot of the difference between the experimental and the fitted values of the absorbance as a function of the distance to the rotation axis.

at the lower of these three concentrations, F2 was shown to be essentially monomeric (see above), this indicates that the NOESY spectra depend mainly on the properties of monomeric F2. These spectra do not show any cross-peak in the amide region (Figure 4). In contrast, the NH−CαH proton region of the spectrum is well populated and shows very little dispersion. This is consistent with the absence of stable secondary structures such as α-helices, β-turns, and β-sheets. Only a few NOEs are present in the aliphatic region (data not shown) compared to what can be expected for a structured protein of 101 residues. This indicates the absence of strong side-chain interactions. These results confirm previous work which had shown that the F2 chemical shifts for each residue type are very similar to the values predicted for a random-coil conformation and that the unusually broad signals for a protein of such a size are due to chemical exchange phenomena between different structures (Chaffotte et al., 1991).

Determination of a Lower Limit for the Bulk Proton Exchange Protection Factor by Magnetization-Transfer Experiments at Neutral pH. The low resolution of the 2D NMR spectra of F2 and the low sensitivity caused by short T_2 relaxation times forbid the assignment of the signals, at least by homonuclear NMR techniques. Hence, it is not possible to determine individual amide exchange rates, to relate them to individual residues of the F2 fragment, and

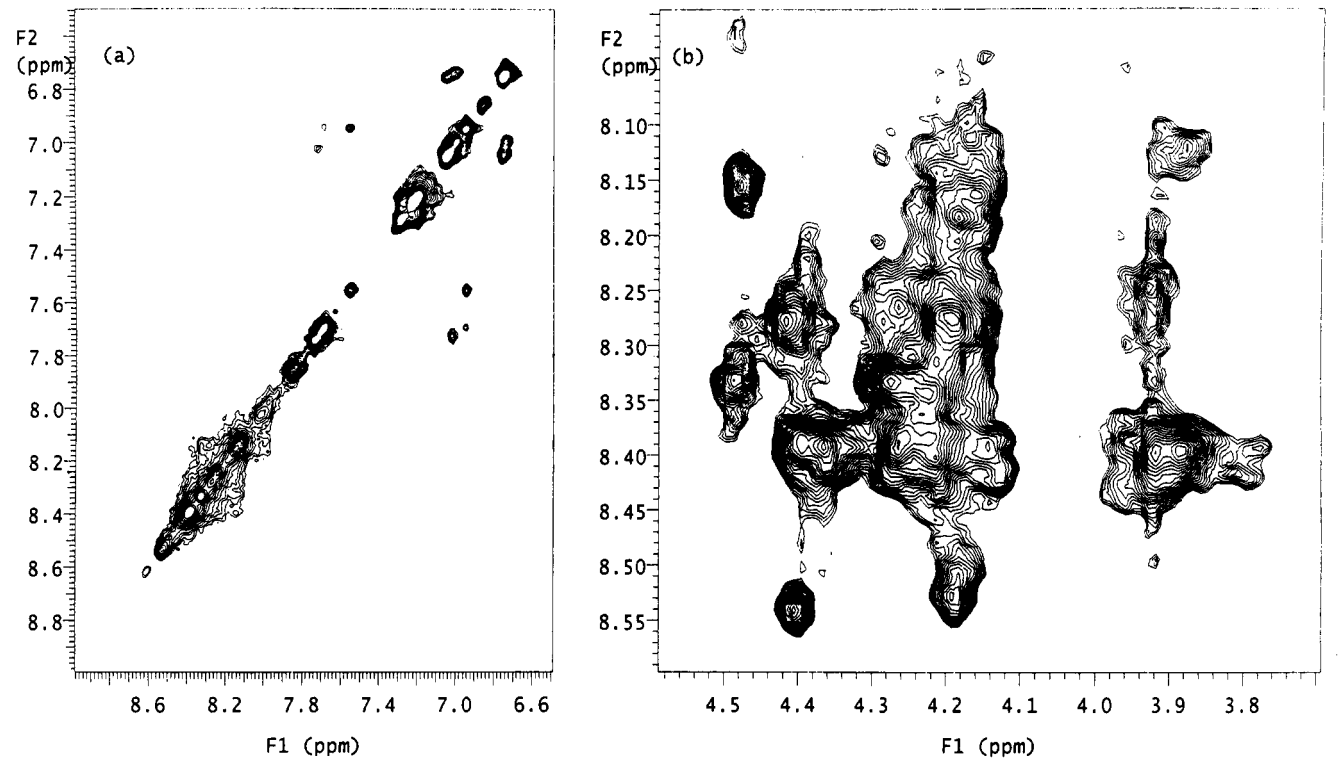

FIGURE 4: Fingerprint regions of the NOE spectrum of F2 (0.85 mM). The spectrum was recorded in buffer B at 0 °C without presaturation as described in Materials and Methods using a modified NOESY sequence (Sodano & Delepierre, 1993a). The residual water signal was suppressed by a time domain data convolution difference technique in the t_2 dimension (Sodano & Delepierre, 1993b). (a) Amide and aromatic regions, and (b) NH−C_αH region. Cross-peaks in (a) can be imputed to dipolar correlations of His, Phe, and Tyr aromatic protons.

to calculate individual protection factors. However, a bulk amide proton exchange rate can be determined from 1D spectra using the magnetization-transfer technique of Spera et al. (1991). Such magnetization-transfer experiments were therefore carried out on the F2 fragment. Experiments were performed at two different pH values (7.8 and 7.0) to eliminate the contribution of cross relaxation to magnetization transfer (Spera et al., 1991). This can be done only if the conformation of the protein is the same at both pHs. For F2, the CD spectra at pH 7.0 and 7.8 (not shown) can be superimposed. In addition, the aliphatic regions of F2 NOESY spectra acquired at both pHs are almost identical (not shown). However, some slight differences are visible in the amide and aromatic regions of the NMR spectra (Figure 5). These may be due to the titration of His residues and to changes in line shape that reflect different exchange rates with water or/and small local differences in conformation. Consequently, in spite of these slight differences in the amide and aromatic regions, the conformations of F2 at pH 7.0 and 7.8 appear very similar, and experiments at these pHs can be used to deduce the contribution of cross-relaxation phenomena.

In order to calculate bulk exchange rates, the mean T_1 spin−lattice relaxation time of the amide protons in the absence of exchange must be determined (Spera et al., 1991). This could not be determined for F2 because all its amide protons exchange rapidly at neutral pH. In addition, F2 forms insoluble aggregates in the pH range from 3.0−3.5 to 6.0−6.5 where exchange rates would be smaller and the exchange contribution to spin relaxation would be negligible. As the true T_1 is expected to be greater than the apparent T_1*, exchange rates derived from eq 1 might be overestimated. However, using the experimental apparent mean T_1* value in eq 1 can provide a lower limit for the protection factor (because it will lead to an overestimated value of the bulk exchange rate). The apparent mean T_1* value was measured at 0 °C, where the contribution of exchange with water is minimized. It was found to be 0.27 ± 0.05 s and provided an apparent bulk exchange rate constant of 0.65 s^{-1} and a protection factor of 12 (Table 3).

Table 3: Experimental and Theoretical Bulk Exchange Rates and Protection Factors for the F2 Fragment[a]

temperature (°C)	T_1* (s)	k_e (s^{-1})	k_{esu} (s^{-1})	lim_{up} (s^{-1})	lim_{lw} (s^{-1})	P_1	P_2
0	0.27	0.65	5.0	70	0.19	12	∞
20	0.39	3.3	28.4	49	0.13	13	80
25	0.39	4.5	42.3	49	0.13	15	62

[a] T_1* is the mean of the amide nonselective spin−lattice relaxation times used for exchange rate calculations; k_e is the experimental bulk exchange rate; k_{esu} is the predicted exchange rate that would be determined experimentally if all F2 amide protons were totally unprotected; lim_{up} and lim_{lw} are the upper and lower rate limits of the method; P_1 and P_2 are respectively the protection factors that should be applied to all the amide protons of F2 or to the 48 amide protons of F2 that are involved in helical structures within the context of the $\alpha_2\beta_2$ complex crystal (Hyde et al., 1988) to reproduce the experimental k_e values. Exchange rates, upper and lower limits of the method, and protections factors were calculated as described in Materials and Methods. All values are reported at pH 7.8.

Bulk exchange rates were also determined at 20 and 25 °C. For this purpose, the T_1* value obtained at 0 °C was scaled to 20 and 25 °C with the appropriate factor derived from the aromatic proton T_1 values at 0 and 25 °C (0.39 s). Table 3 summarizes the results obtained. It can be seen that regardless of the temperature, the experimental bulk exchange rate (k_e) is always smaller, at least by a factor of 7.7, than the predicted rate if all F2 amide protons exchanged at their

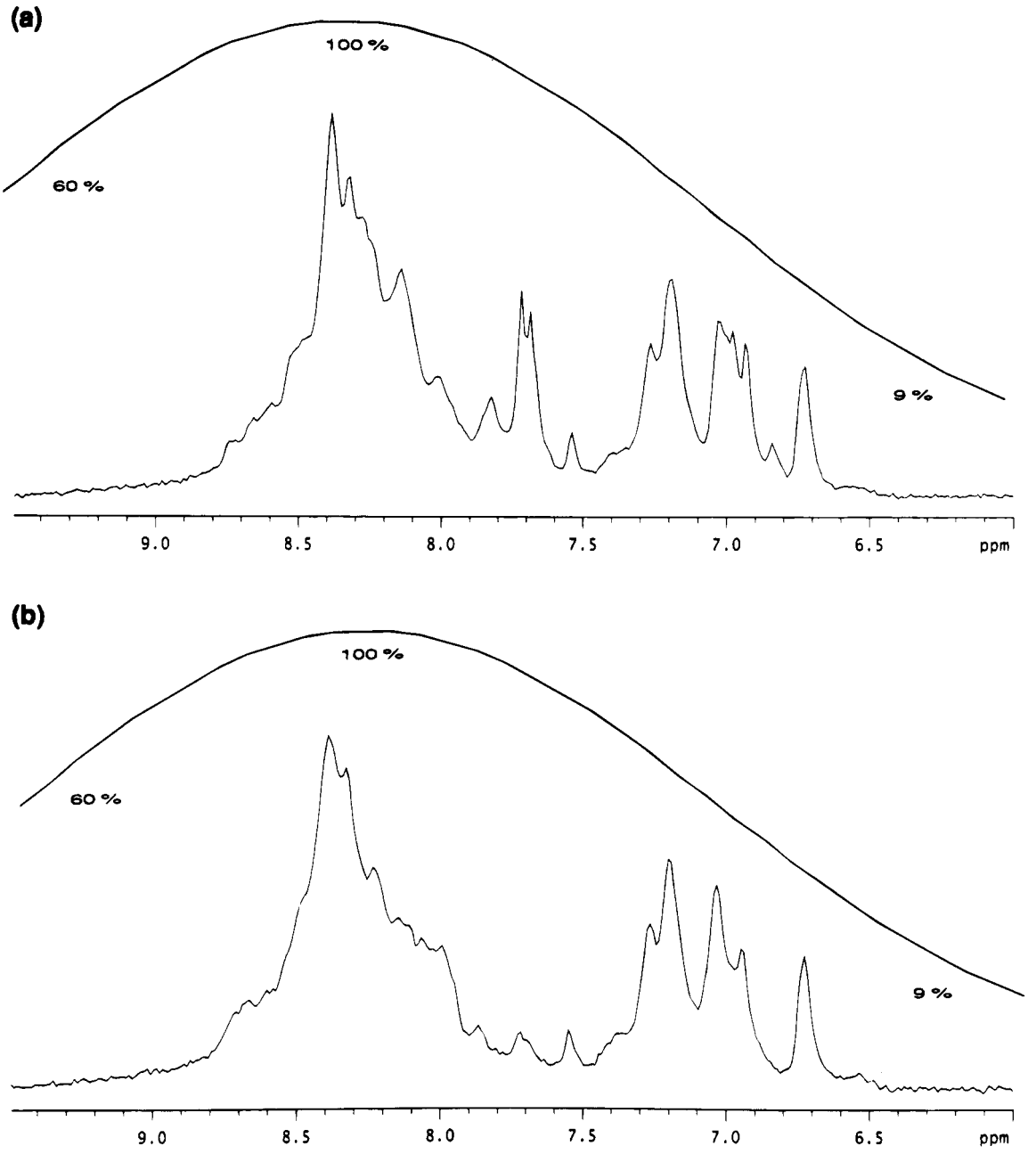

FIGURE 5: Low-field region of the 1D spectra of F2 at (a) pH 7.8 and (b) pH 7.0 at 0 °C. Both spectra were acquired with an 11-echo pulse scheme without presaturation (Sklenár & Bax, 1987). The continuous line above each of the spectra represents the theoretical excitation profile.

intrinsic rate (k_{esu}). This unambiguously demonstrates that at least some F2 amide protons are protected against exchange. It should be noted that, at each temperature investigated, the k_{esu} value falls between the lower (lim_{lw}) and upper (lim_{up}) limits of the method employed (see Materials and Methods).

To get further insight into how much these protons are protected, the protection factor that should be applied to amide exchange rates to reproduce experimental results was determined. For this purpose, eq 5 was used. If protection is considered for all amide protons, very small though significant protection factors (P_1 in Table 3) are obtained. They are in the range of 12−15 and appear to vary very little with temperature between 0 and 25 °C.

In summary, these experiments unambiguously demonstrate that F2 possesses amide protons that are protected against exchange and show that the bulk protection factor would be of the order of 10 if the protection were distributed among all the amide protons. As discussed below, this value represents a lower limit for the bulk protection factor.

Determination of an Upper Limit for the Bulk Protection Factor by Magnetization Transfer and Isotope-Exchange Experiments at Neutral pH. The magnetization-transfer experiments described in the previous section can also provide a first estimate of an upper limit for the bulk protection factor. Indeed, the bulk protection factor needed to reproduce the magnetization-transfer results is expected to increase when the postulated number of protected protons decreases. Setting a lower limit to the number of amide protons that are protected in F2 should therefore provide an upper limit for the bulk protection factor. Thus, let us assume that only 50% of the amide protons of F2 are

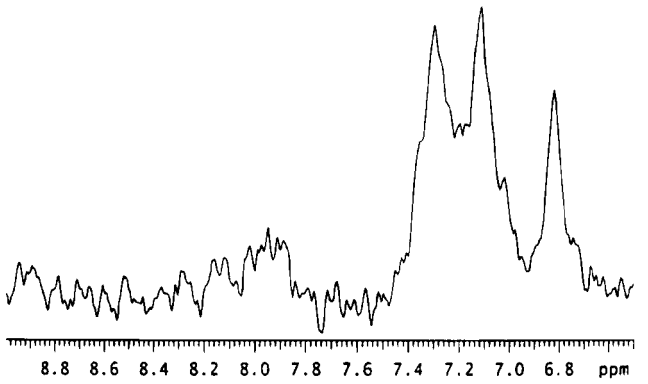

FIGURE 6: Low-field region of the 1D spectrum of F2 at 0 °C in buffer B prepared in D_2O (pD 7.4). The spectrum was recorded with eight accumulations after 90 s of exchange. Protein concentration was 0.1 mM. Observed signals correspond to aromatic protons of His, Phe, and Tyr residues. Broad signals at 8.14 and 8.02–7.84 ppm belong to H_2 protons of His.

protected against exchange. This value was chosen because it is compatible with the amount of secondary structure of F2 estimated from CD as well as with the assumption that protection would exist only for the 48 F2 amide protons that form α-helices in the native $\alpha_2\beta_2$ complex, while the other 48 amide protons would exchange at their intrinsic rates. Protection factors for 50% of protected amide protons (P_2) were therefore computed as described in Materials and Methods, using eq 6. Results are reported in Table 3. As expected, higher protection factors (P_2) are obtained with only 50% of the protons protected than if all F2 amide protons are assumed to be protected (P_1). It is important to note, however, that if only 50% or fewer of the amide protons were taken as protected, the exchange rate observed experimentally at 0 °C was always significantly smaller than the rates simulated with eq 6 whatever the protection factor used in the simulation. Indeed, at 0 °C, the experimental k_e was 0.65 s^{-1} and the lower limit for k_{esu} obtained with an "infinite" P_2 was 1.56 s^{-1}. This type of simulation was repeated considering different sets of 48 amide protons of F2 to be protected, and again, experimental exchange rates could not be simulated. Thus, even if an infinite protection factor (P_2) was used, the experimental exchange rates could not be reproduced for 50% of protected protons. This suggested that protection exists for significantly more than 50% of the amide protons, and that the bulk protection factor must be below the upper limits (P_2) reported in Table 3.

Unfortunately, in the magnetization-transfer experiments described above, it was not possible to determine how many protons were protected, which precluded a more precise evaluation of the bulk protection factor. Therefore, direct isotope-exchange experiments were performed in an attempt to get a better estimate of the upper limit for the protection factors. Experiments were carried out at low protein concentration (0.1 mM). Fully protonated F2 was lyophilized and dissolved at 0 °C in buffer B prepared in D_2O (pD 7.4 at 0 °C). 1D spectra were recorded immediately. No NH could be detected in the first spectrum recorded with 8 scans, that is, only 90 s after dissolution (Figure 6). Furthermore, the amide and aromatic regions remained constant in the spectra recorded after 132 s (32 scans) and 189 s (64 scans), and in spectra recorded after 30 min with better signal to noise ratios. Thus, no detectable NH proton was present after 90 s of exchange.

The experimental conditions were chosen to minimize aggregation (low concentration) and to reduce the experiment dead time (accumulation of only 8 scans). They resulted, however, in a low signal to noise ratio in the spectrum acquired at 90 s. Quantitative measurements on a single amide proton, or a fraction of it, might therefore be quite imprecise. This was not critical, however, since the amide region of the F2 1D spectrum is very crowded and there is not a single chemical shift at which there is only one amide proton resonance (see Figure 5). The broad His aromatic signals could actually be observed and quantified in the 90-s spectrum even though their intensity (height) was close to the noise upper limit (Figure 6). Thus, a peak with an intensity as low as the maximum of the noise intensity could be reliably detected after 90 s. Therefore, the maximum of the noise intensity was taken as the minimum peak intensity that can be observed in the 90-s spectrum.

Using this limit, the minimum exchange rate was determined in a spectral region corresponding to approximately 60% of the amide protons. It was found to be 26.5×10^{-3} s^{-1}. As the initial intensity was estimated using the lowest intensity peak in the envelope containing 60% of the residues (peak at 8.24 ppm), this value represents a safe lower limit of the exchange rate constant. This result, in combination with the mean of the intrinsic exchange rates at 0 °C and a corrected pD of 7.8 (k_{th} = 1.587 s^{-1}), was used to calculate an upper limit for the mean protection factor for the 60% of the amides that were analyzed in this experiment. The upper limit obtained was 60. It is rather unlikely that the exchange rate distribution for the remaining 40% of the protons could be largely different, and it seems reasonable to extrapolate this value of 60 to basically all F2 amide protons. Thus the upper limit for the protection factor determined by direct isotope exchange can be conservatively set to 60. It should be emphasized that all the assumptions made underestimated the exchange rates so as to establish a safe upper limit for the protection factors.

DISCUSSION

The results obtained in the present study can be summarized as follows. In a buffer where the β_2 subunit of tryptophan synthase folds efficiently and is very stable, its isolated C-terminal F2 domain spontaneously folds into a conformation which provides only a weak protection of its amide protons and shows no NOEs typical of secondary structures. Yet it appears to contain significant amounts of secondary structure according to its CD as well as its FTIR spectra.

The amounts of secondary structure predicted from far-UV CD spectra are usually fairly precise as far as α-helices are concerned, but rather unreliable for β-structures. This is verified in the case of the isolated F2 fragment for which the amount of α-helix estimated in the present study is close to that obtained previously using a different deconvolution method, while the present estimate for β-structures is quite different from that (34%) obtained previously (Chaffotte et al., 1991). The values reported in Table 1 (21% of α-helix and about 23% of β-structure) will be used for further discussion. The amount of β-structure predicted from the FTIR spectra is smaller than, but still comparable to, that obtained from the far-UV CD spectrum (Tables 1 and 2). Though FTIR is usually more precise than CD for estimating

β-structure contents, it still should be considered as providing only approximations of the absolute amount of secondary structure. This is particularly true for α-helices, because it is difficult to separate the overlapping absorption bands of unordered and α-helical structures (Surewicz et al., 1993). Hence, the amount of α-helix cannot be estimated from the FTIR spectrum of F2. Nevertheless, the position of the major absorption band of F2 at 1647 cm^{-1} (just halfway between the values for unordered peptides and for α-helices) is a good indication of the presence of significant amounts of α-helix in F2. Thus, within the reliability of both methods, FTIR and CD provide similar information on the presence of secondary structure in F2.

More important is the novel observation that the FTIR spectra of isolated F2 exhibit typical absorption bands that unambiguously reflect the presence of amide protons involved in hydrogen bonds of authentic secondary structures. Why, then, does NMR fail to detect nuclear Overhauser effects characteristic of such secondary structures in F2? These NOEs may be missing from the spectrum because of a high conformational mobility of F2, resulting in averaging on the chemical shift time scale and in line broadening. Indeed, the random coil-like chemical shifts in F2 NMR spectra indicate fast exchange on the chemical shift time scale, showing that the lifetime for a proton in any particular chemical environment is in the millisecond range or shorter (Jardetzky & Roberts, 1981). Also, the line broadening observed for F2, which corresponds to intermediate exchange on the spin−spin relaxation time scale, is indicative of interconversion of different molecular forms in the millisecond time range. Averaging on the chemical shift time scale and line broadening have also been reported for the molten globule state of α-lactalbumin (Alexandrescu et al., 1993). However, for this protein, sequential NH_i-NH_{i+1} NOEs characteristic of α-helices were observed. The absence of NOEs characteristic of α-helices, β-sheets, and turns in F2 NOESY spectra (even at 0 °C) may thus indicate the existence of interconversion phenomena that are fast relative to the millisecond range.

All the NMR parameters of F2 are compatible with the existence of rapidly interconverting conformations. Indeed, the very poor chemical shift dispersion, the absence of detectable structure-induced chemical shifts, the absence of NH−NH NOE connectivities, the presence of only a few NOEs between side-chain protons, and the broad signals caused by chemical exchange phenomena all point to a rapid conformational equilibrium with no preferred conformation.

This conclusion is supported by the proton-exchange data. Indeed, direct isotope exchange experiments performed at 0 °C showed that the average protection factor was at most 60. Yet, *even with infinite protection factors*, it was impossible to account for the magnetization-transfer results obtained at 0 °C when assuming that 50% or less of the amide protons are protected (Table 3). In fact, about 75% of the residues must be assumed to be involved in secondary structures if one wants to account for the magnetization-transfer results at 0 °C with a protection factor of 60. Because the CD spectrum of F2 hardly changes with temperature between 5 and 25 °C (unpublished results), the same is likely to hold at 25 °C, too. As a consequence, the bulk protection factor must be closer to 12−15, the values obtained at 0 and 25 °C when averaging over all the amide protons of F2 (Table 3), than to 60. Such a small protection factor would certainly not be expected if the secondary structures detected by CD and FTIR were stable and rigid.

Thus, when isolated from the context of the entire β_2 subunit, F2 appears as a molten globule with 30−45% of its residues involved in secondary structures that (i) are stabilized by the usual hydrogen bonds involving amide protons, (ii) are rapidly fluctuating, and (iii) are distributed along the major part of the polypeptide chain. Therefore, non-native secondary structures also must be present in F2. It should be pointed out that, though studied here in the absence of any denaturing agent, the F2 fragment appears to be in a more fluctuating conformational state than other well-characterized equilibrium folding intermediates such as the A state of α-lactalbumin (Alexandrescu et al., 1993; Chyan et al., 1993; Baum et al., 1989) and the I form of apomyoglobin (Hughson et al., 1990).

The properties of isolated F2 will now be compared to those of early folding intermediates. F2 folds in less than 4 ms into a conformation that exhibits a far-UV CD spectrum and ANS binding properties similar to those of the "burst" intermediates observed within the first milliseconds of the folding of several proteins (Chaffotte et al., 1992a). Moreover, folded F2 is not in a "dead end" on the folding pathway since addition of the complementary F1 fragment restores the native conformation. Finally, as observed by pulsed proton exchange for other burst intermediates, it shows little protection of its amide protons. From the value estimated for the bulk protection factor, one can predict the outcome of pulsed proton exchange experiments as they are usually performed to characterize early folding intermediates. Let us consider, for instance, an 8.4-ms pulse at 20 °C and pH 9.5 as used for studies on the folding of hen egg white lysozyme (Radford et al., 1992). One can estimate the fraction of each amide proton that would be exchanged at the end of such a pulse, using the intrinsic exchange rate constants (Bai et al., 1993; Connelly et al., 1993) divided by the postulated protection factor. Hence, for the amide protons that belong to secondary structures in native lysozyme, an average proton occupancy of about 73% would be predicted using a protection factor of 10. These values are to be compared with the average values of about 77% and 93% observed respectively for α-helices and β-strands at early stages of lysozyme folding (Radford et al., 1992). Thus a protection factor of 10, as estimated for the F2 amide protons, would result in a proton protection for lysozyme intermediates not very different from that observed experimentally. Similar calculations performed on the F2 fragment yield similar predictions, with about 70% proton occupancies predicted at the end of a pulse. The fraction of the amide protons of F2 that would be protected against exchange during a pulsed proton exchange experiment would therefore be relatively small and indeed compatible with what is usually observed for early folding intermediates (Roder et al., 1988; Udgaonkar & Baldwin, 1988, 1990; Bycroft et al., 1990; Radford et al, 1992; Briggs & Roder, 1992; Mullins et al., 1993; Varley et al., 1993; Jacobs & Fox, 1994).

From its rate of folding, its far-UV CD spectrum, its ANS binding, and its proton exchange properties, F2 appears as very similar to the commonly observed burst intermediates and may therefore serve as an appropriate model to understand the apparent contradiction between the CD spectra and the pulsed proton exchange properties of such intermediates. That F2 has authentic secondary structures stabilized by

hydrogen bonds, as demonstrated by the FTIR results, clearly rules out the first of the three hypotheses proposed to solve this contradiction, according to which non-hydrogen-bonded repetitive conformations of the polypeptide backbone might have given rise to the far-UV ellipticity signal. The second hypothesis, i.e., that the secondary structure present under the folding conditions could be disrupted under the alkaline conditions of the pulse, is also ruled out since we showed that the secondary structure of F2 is stable at pH 9.5. The third hypothesis, i.e., that authentic secondary structure elements might fail to provide a significant protection of their amide protons during a pulsed proton exchange experiment, is on the contrary strongly supported by our experimental results.

That F2 contains authentic hydrogen-bonded secondary structure elements strongly suggests that the early folding intermediates with large far-UV CD signals but little protection of their amide protons indeed contain real secondary structures. They are therefore the earliest structured intermediates thus far identified. It should be pointed out, however, that, as discussed above, non-native secondary structures seem to also exist in this rapidly fluctuating population of intermediates, suggesting that off-pathway conformations are also present at this very early stage of the folding process. Why are secondary structure elements stabilized in these intermediates as compared to short peptides in aqueous solution? To what extent are native motifs predominantly present within these intermediates? These are probably the most important and challenging questions that have to be solved for understanding the basic mechanisms of protein folding.

ACKNOWLEDGMENT

We thank Dr. Thierry Rose for his help in the implementation of the VARSLC1 algorithm.

REFERENCES

Alexandrescu, A. T., Evans, P. A., Pitkeathly, M., Baum, J., & Dobson, C. M. (1993) *Biochemistry 32*, 1707−1718.
Bai, Y., Milne, J. S., Mayne, L., & Englander, S. W. (1993) *Proteins: Struct. Funct., Genet. 17*, 75−86.
Baldwin, R. L. (1993) *Curr. Opin. Struct. Biol. 3*, 84−91.
Baldwin, R. L., & Roder, H. (1991) *Curr. Biol. 1*, 218−220.
Baum, J., Dobson, C. M., Evans, P. A., & Hanley, C. (1989) *Biochemistry 28*, 7−13.
Bradford, M. M. (1976) *Anal. Biochem. 72*, 248−254.
Briggs, M., & Roder, H. (1992) *Proc. Natl. Acad. Sci. U.S.A. 89*, 2017−2021.
Bycroft, M., Matouschek, A., Kellis, J. T., Jr., Serrano, L., & Fersht, A. R. (1990) *Nature 346*, 488−490.
Cameron, D. G., & Moffatt, D. J. (1984) *J. Test. Eval. 12*, 78−85.
Cameron, D. G., & Moffatt, D. J. (1987) *Appl. Spectrosc. 41*, 539−544.
Chaffotte, A. F., Guillou, Y., Delepierre, M., Hinz, H., & Goldberg, M. E. (1991) *Biochemistry 30*, 8067−8073.
Chaffotte, A. F., Cadieux, C., Guillou, Y., & Goldberg, M. E. (1992a) *Biochemistry 31*, 4303−4308.
Chaffotte, A. F., Guillou, Y., & Goldberg, M. E. (1992b) *Biochemistry 31*, 9694−9702.
Chyan, C. L., Wormald, C., Dobson, C. M., Evans, P. A., & Baum, J. (1993) *Biochemistry 32*, 5681−5691.
Connelly, G. P., Bai, Y., Jeng, M., & Englander, S. W. (1993) *Proteins: Struct., Funct., Genet. 17*, 87−92.
Elöve, G. A., Chaffotte, A. F., Roder, H., & Goldberg, M. E. (1992) *Biochemistry 31*, 6876−6883.
Englander, S. W., Downer, N. W., & Teitelbaum, H. (1972) *Annu. Rev. Biochem. 41*, 903−924.
Friguet, B., Djavadi-Ohaniance, L., & Goldberg, M. E. (1989) *Res. Immunol. 140*, 355−376.
Hennessey, J. P., Jr., & Johnson, W. C., Jr. (1981) *Biochemistry 20*, 1085−1094.
Högberg-Raibaud, A., & Goldberg, M. E. (1977) *Biochemistry 16*, 4014−4020.
Hughson, F. M., Wright, P. E., & Baldwin, R. L. (1990) *Science 249*, 1544−1548.
Hyde, C. C., Ahmed, S. E., Padlan, E. A., Miles, E. W., & Davies, D. R. (1988) *J. Biol. Chem. 263*, 17857−17871.
Jackson, M., & Mantsch, H. H. (1991) *Can. J. Chem. 69*, 1639−1642.
Jacobs, M. D., & Fox, R. O. (1994) *Proc. Natl. Acad. Sci. U.S.A. 91*, 449−453.
Jardetzky, O., & Roberts, G. C. K. (1981) in *NMR in Molecular Biology*, pp 116−120, Academic Press, Inc., London.
Jennings, P. A., & Wright, P. E. (1993) *Science 262*, 892−896.
Kaufmann, M., Schwarz, T., Jaenicke, R., Schnackerz, K. D., Meyer, H. E., & Bartholmes, P. (1991) *Biochemistry 30*, 4173−4179.
Kuwajima, K. (1989) *Proteins: Struct., Funct., Genet. 6*, 87−103.
Manavalan, P., & Johnson, W. C., Jr. (1987) *Anal. Biochem. 167*, 76−85.
Mullins, L. S., Pace, C. N., & Raushell, F. M. (1993) *Biochemistry 32*, 6152−6156.
Pauling, L., & Corey, R. B. (1951a) *Proc. Natl. Acad. Sci. U.S.A. 37*, 235−250.
Pauling, L., & Corey, R. B. (1951b) *Proc. Natl. Acad. Sci. U.S.A. 37*, 251−256.
Plateau, P., & Guéron, H. (1982) *J. Am. Chem. Soc. 104*, 7310−7311.
Radford, S. E., Dobson, C. M., & Evans, P. A. (1992) *Nature 358*, 302−307.
Roder, H., Elöve, G. A., & Englander, S. W. (1988) *Nature 335*, 700−704.
Rohl, A. C., Scholtz, J. M., York, E. J., Stewart, J. M., & Baldwin, R. L. (1992) *Biochemistry 31*, 1263−1269.
Sklenár, V., & Bax, A. (1987) *J. Magn. Reson. 74*, 469−479.
Sodano, P., & Delepierre, M. (1993a) *J. Biomol. NMR 3*, 471−477.
Sodano, P., & Delepierre, M. (1993b) *J. Magn. Reson. 104*, 88−92.
Spera, S., Ikura, M., & Bax, A. (1991) *J. Biomol. NMR 1*, 155−165.
Surewicz, W. K., & Mantsch, H. H. (1988) *Biochem. Biophys. Acta 952*, 115−130.
Surewicz, W. K., Mantsch, H. H., & Chapman, D. (1993) *Biochemistry 32*, 389−394.
Udgaonkar, J. B., & Baldwin, R. L. (1988) *Nature 335*, 694−699.
Udgaonkar, J. B., & Baldwin, R. L. (1990) *Proc. Natl. Acad. Sci. U.S.A. 87*, 8197−8201.
Varley, P., Gronenborn, A. M., Christensen, H., Wingfield, P. T., Pain, R. H., & Clore, G. M. (1993) *Science 260*, 1110−1113.
Yang, J. T., Wu, C.-S., & Martínez, H. M. (1986) *Methods Enzymol. 130*, 208−269.

BI9422642